DIAGNOSTIC NEURORADIOLOGY

Right entorhinal cortical thickness is associated with Mini-Mental State Examination scores from multi-country datasets using MRI

Koji Yamashita[1] · Takahiro Kuwashiro[2] · Kensuke Ishikawa[3] · Kiyomi Furuya[1] · Shino Harada[1] · Seitaro Shin[1] · Noriaki Wada[1] · Chika Hirakawa[4] · Yasushi Okada[2] · Tomoyuki Noguchi[1]

Abstract

Purpose To discover common biomarkers correlating with the Mini-Mental State Examination (MMSE) scores from multi-country MRI datasets.

Methods The first dataset comprised 112 subjects (49 men, 63 women; range, 46–94 years) at the National Hospital Organization Kyushu Medical Center. A second dataset comprised 300 subjects from the Alzheimer's Disease Neuroimaging Initiative (ADNI) database (177 men, 123 women; range, 57–91 years). Three-dimensional T1-weighted MR images were collected from both datasets. In total, 14 deep gray matter volumes and 70 cortical thicknesses were obtained from MR images using FreeSurfer software. Total hippocampal volume and the ratio of hippocampus to cerebral volume were also calculated. Correlations between each variable and MMSE scores were assessed using Pearson's correlation coefficient. Parameters with moderate correlation coefficients ($r > 0.3$) from each dataset were determined as independent variables and evaluated using general linear model (GLM) analyses.

Results In Pearson's correlation coefficient, total and bilateral hippocampal volumes, right amygdala volume, and right entorhinal cortex (ERC) thickness showed moderate correlation coefficients ($r > 0.3$) with MMSE scores from the first dataset. The ADNI dataset showed moderate correlations with MMSE scores in more variables, including bilateral ERC thickness and hippocampal volume. GLM analysis revealed that right ERC thickness correlated significantly with MMSE score in both datasets. Cortical thicknesses of the left parahippocampal gyrus, left inferior parietal lobe, and right fusiform gyrus also significantly correlated with MMSE score in the ADNI dataset ($p < 0.05$).

Conclusion A positive correlation between right ERC thickness and MMSE score was identified from multi-country datasets.

Keywords Entorhinal cortex · Mini-Mental State Examination · MRI · ADNI

✉ Koji Yamashita
yamakou@radiol.med.kyushu-u.ac.jp

Takahiro Kuwashiro
kuwashiro.takahiro.vy@mail.hosp.go.jp

Kensuke Ishikawa
ishikawa.kensuke.fw@mail.hosp.go.jp

Kiyomi Furuya
furuya.kiyomi.uw@mail.hosp.go.jp

Shino Harada
haradashi0629@gmail.com

Seitaro Shin
ss_masajirou@yahoo.co.jp

Noriaki Wada
tstw.grace128@gmail.com

Chika Hirakawa
tstw.grace128@gmail.com

Yasushi Okada
okada.yasushi.yh@mail.hosp.go.jp

Tomoyuki Noguchi
tnogucci@radiol.med.kyushu-u.ac.jp

[1] Department of Radiology, Clinical Research Institute, National Hospital Organization Kyushu Medical Center, 1-8-1 Jigyohama, Chuo-ku, 810-0065 Fukuoka, Japan

[2] Department of Cerebrovascular Medicine and Neurology, National Hospital Organization Kyushu Medical Center, 1-8-1 Jigyohama, Chuo-ku, 810-0065 Fukuoka, Japan

[3] Department of Psychiatry, Clinical Research Institute, National Hospital Organization Kyushu Medical Center, 1-8-1 Jigyohama, Chuo-ku, 810-0065 Fukuoka, Japan

[4] Department of Medical Technology, Division of Radiology, National Hospital Organization Kyushu Medical Center, 1-8-1 Jigyohama, Chuo-ku, Fukuoka 810-0065, Japan

Abbreviations

AD	Alzheimer's disease
ADNI	Alzheimer's Disease Neuroimaging Initiative
ANOVA	Analysis of variance
ASHS	Automated segmentation of hippocampal subfields
BA	Brodmann area
ERC	Entorhinal cortex
GLM	General linear model
MCI	Mild cognitive impairment
MMSE	Mini-Mental State Examination
MMSE-J	Mini-Mental State Examination Japanese version
MTL	Medial temporal lobe
PHC	Parahippocampal cortex

Introduction

Medial temporal lobe (MTL) atrophy is highly associated with cognitive performance. Neurofibrillary tangle deposition is initially seen in the transentorhinal region, while any cognitive impairments are not clinically evident at this stage [1]. The entorhinal cortex (ERC) is the key feature of Braak stage III, which is closely associated with cognitive impairment [1]. The ERC is located medial to the rhinal sulcus and comprises the anterior portion of the parahippocampal gyrus. The ERC functions as the crucial gateway between the hippocampus and neocortex [2, 3]. Thickness of the ERC is known to correlate with the effects of β-amyloidosis and tauopathic neurodegeneration [4, 5]. Damage to the ERC has been shown to impair cognitive function [3, 6, 7]. In addition, loss and atrophy of layer II ERC neurons are associated with memory test performance and are seen in elderly individuals preceding the onset of dementia symptoms [6].

Magnetic resonance imaging (MRI) is the most frequently utilized non-invasive technique for computing brain volume with high reproducibility. Morphological evaluation using MRI has revealed relationships between cortical thickness and cognitive test performance in healthy individuals, irrespective of scan sessions, scanners, or field strengths [8, 9].

The Mini-Mental State Examination (MMSE) is the most commonly used tool in screening for cognitive impairment. MMSE provides reliable scores without being influenced by repetition or learning, and consistent results can be obtained by the same or different examiners on repeat testing [10]. Many human studies have demonstrated that MMSE scores correlate with ERC thickness or volumes [11–18]. Long et al. found the loss of asymmetry in ERC has been shown as biomarkers to identify preclinical Alzheimer's disease (AD) [19]. Thus, right and left ERC thicknesses should have different strength of association with MMSE scores. Subfield analysis of MTL has been investigated to perform a detailed

evaluation of MTL subregions, and the analysis has offered insight into the early diagnosis and monitoring of AD [13]. However, the relevance between MMSE scores and ERC thickness in multi-country datasets remains unknown. The Alzheimer's Disease Neuroimaging Initiative (ADNI) is an open data sharing framework and the largest database of elderly subjects in the USA [20].

The present study aimed to discover common biomarkers correlating with MMSE scores using MRI datasets from both National Hospital Organization Kyushu Medical Center (KMC) and the ADNI.

Materials and methods

Dataset from KMC

This study was approved by the institutional review board of KMC. The requirement for informed consent for study participation was waived due to the retrospective nature of this study. Data from 200 consecutive patients (90 men, 110 women; median age, 77 years; range, 36–95 years) who underwent MRI between February 2019 and August 2020 were retrospectively analyzed. Among these, subjects who underwent testing using the Japanese version of the MMSE (MMSE-J) were included in the present study. Exclusion criteria were as follows: (i) patients with severe head motion artifacts; or (ii) patients with treatable dementias such as idiopathic normal-pressure hydrocephalus, brain tumor, metabolic, infectious, inflammatory, or drug-induced cognitive impairment, or history of stroke other than small vessel disease. Motion artifact and the presence of intracranial abnormality on the MR images were evaluated by an experienced radiologist (K.Y.).

Three-dimensional (3D) T1-weighted imaging was performed using a 1.5-T MRI unit (Magnetom Symphony Tim, Siemens, Erlangen, Germany) with a 6-channel head coil. The following scanning parameters were used: repetition time, 1700 ms; echo time, 3.4 ms; inversion time, 800 ms; flip angle, 15°; 144 sagittal sections; slice thickness = 1.25 × 1.25 × 1.25 mm³; field of view, 230 × 230 mm²; matrix, 256 × 256.

Dataset from the ADNI database

Images from 3D T1-weighted MRI were collected from the ADNI database (http://adni.loni.usc.edu/). The representative voxel resolution of ADNI (ADNI1) data was 1 × 1 × 1.2 mm³. The dataset comprised 300 subjects (177 men, 123 women; median age, 76 years; range, 57–91 years). These subjects comprised 100 subjects each for normal controls, mild cognitive impairment (MCI), and AD.

Preprocessing of 3D T1-weighted images from the two datasets using the FreeSurfer pipeline
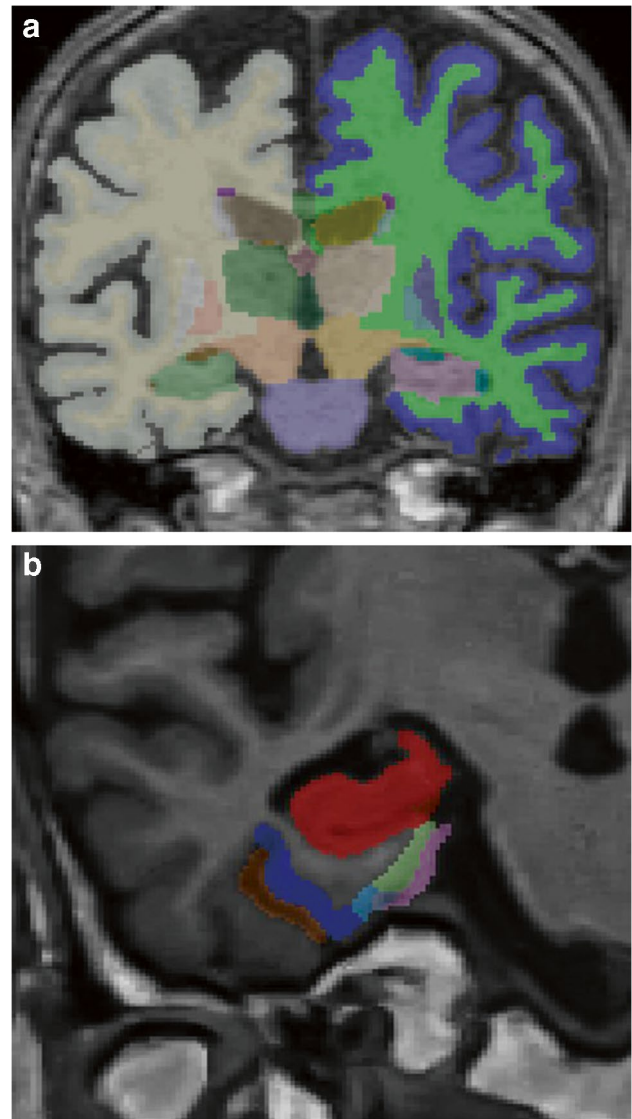
All MR images from the two datasets were preprocessed with the FreeSurfer pipeline (version 6.0.0) [21, 22], a freely available software commonly used for brain structural MRI analysis. The automatic reconstruction steps include non-uniform intensity normalization, automatic subcortical segmentation, resampling of the average curvature from the atlas to subject, cortical parcellation using the Desikan-Killiany cortical atlas [23], and parcellation statistics (https://surfer.nmr.mgh.harvard.edu/fswiki/recon-all). A representative parcellation image is shown in Fig. 1a. A detailed description of the reconstruction steps has been provided elsewhere [22]. The entire cortex of each subject was visually inspected, and the topological defects were manually corrected [24]. Volume data of bilateral hippocampi, amygdalas, thalami, putamina, caudate nuclei, globi pallidi, nuclei accumbentes, and total corpora callosa were collected from the cortical parcellation atlas. Mean cortical thickness of the right hemisphere, left hemisphere, and 70 cortical thicknesses (35 variables in each hemisphere) were also attained from the atlas. Total hippocampal volume and the ratio of hippocampus to the cerebral volume were also calculated. These variables including subject age were used for further analyses.

Preprocessing of 3D T1-weighted images from the two datasets using the automatic segmentation of hippocampal subfields pipeline

All MR images from the two datasets were implemented in the automatic segmentation of hippocampal subfields (ASHS)-Penn Memory Center (PMC)-T1 pipeline (version 1.0.0) [25]. The ASHS-PMC-T1 pipeline consists of multi-atlas algorithm by manual segmentation of the MTL cortex and machine learning techniques. The detailed protocol has been reported elsewhere [13, 25]. Automated segmentation of anterior/posterior hippocampus, ERC, Brodmann areas (BA) 35 and 36, and parahippocampal cortex (PHC) from each subject via ITK-SNAP distributed segmentation service (https://dss.itksnap.org), and volume of each subregion was calculated using ITK-SNAP software (version 3.8.0) [26]. A representative segmentation of MTL subregions is indicated in Fig. 1b.

MMSE

We were interested in testing whether some variables derived from multi-country datasets correlated with MMSE scores. To address this question, subjects who completed the MMSE-J at KMC or the MMSE from ADNI cohorts were included for analysis. The MMSE-J and MMSE were administered to screen for cognitive impairments, with all assessments performed by experienced examiners. MMSE-J

Fig. 1 Representative images of the FreeSurfer automated brain parcellation (**a**) and the automatic segmentation of hippocampal subfields (ASHS-T1) pipeline (**b**).

and MMSE scores were obtained from each subject at KMC and from the ADNI database, respectively.

Statistical analysis

All statistical analyses were performed using PASW Statistics version 18 (SPSS Inc., Chicago, IL, USA) and graphs were plotted in Prism version 7 (GraphPad Software, La Jolla, San Jose, CA, USA).

Correlations between each variable including subject age and MMSE score (MMSE-J at KMC and MMSE from ADNI cohorts) were assessed using Pearson's correlation coefficient. Overfitting occurs when too many variables included in the regression analysis [27, 28]. According

to the literatures, the parameters showing moderate correlation coefficients ($r > 0.3$) [29] from each dataset were then taken as independent variables and evaluated using one-way analysis of variance (ANOVA) with general linear model (GLM) analyses. In addition, thickness of the right ERC was compared with that of the left ERC for both datasets using two-tailed Student's t-tests. Thicknesses of the right and left ERC were compared among normal controls, MCI, and AD from the ADNI dataset using one-way ANOVA followed by Student's t-tests with Bonferroni corrections for multiple comparisons, respectively.

Next, correlations between volume of each MTL subregions and MMSE score were assessed using Pearson's correlation coefficient. Parameters showing moderate correlation coefficients ($r > 0.3$) from each dataset were then taken as independent variables and evaluated using GLM analysis. Volumes of right and left ERC were compared among normal controls, MCI, and AD from the ADNI dataset using one-way ANOVA followed by Student's t-tests with Bonferroni corrections for multiple comparisons, respectively.

Values of $p < 0.05$ were considered indicative of statistical significance in all statistical analyses.

Results

One hundred and twelve subjects from KMC fulfilled the criteria (49 men, 63 women; median age, 77 years; range, 46–94 years). Demographic and clinical information for subjects are presented in Table 1. Mean age did not differ significantly between datasets.

Pearson's correlation coefficients of the dataset from KMC with the FreeSurfer pipeline

Table 2 shows the correlations between MMSE score and values from the KMC dataset. Variables with moderate

correlation coefficients ($r > 0.3$) were thicknesses of the right ERC and right insular cortex, and volumes of the right amygdala and right, left, and total hippocampi. All variables with moderate correlation coefficients showed positive correlations with MMSE scores.

Pearson's correlation coefficients of the ADNI dataset with the FreeSurfer pipeline

Table 3 shows the correlations between MMSE score and values from the ADNI dataset. More variables had moderate correlation coefficients ($r > 0.3$) than KMC dataset as shown in Table 3. All variables with moderate correlation coefficients displayed positive correlations with MMSE scores.

GLM analysis of both datasets with the FreeSurfer pipeline

GLM analysis demonstrated that right ERC thickness correlated significantly with MMSE score for the first dataset ($p = 0.005$; Fig. 2a), and thickness of the right ERC ($p = 0.039$; Fig. 2b), parahippocampal gyrus ($p = 0.023$), left inferior parietal lobe ($p = 0.025$), and right fusiform gyrus ($p = 0.035$) for the ADNI dataset. Figure 2 shows scatter plots and linear regression lines for right ERC thickness from both datasets.

Differences in right and left ERC thickness

The dataset from KMC exhibited that the right ERC tended to be thicker (mean ± standard deviation [SD] = 3.07 ± 0.54 mm) than the left ERC (mean = 3.00 ± 0.49 mm), although the difference was not significant ($p = 0.0663$; Fig. 3a). In the ADNI dataset, the right ERC was significantly thicker (mean = 2.81 ± 0.47 mm) than the left ERC (mean = 2.70 ± 0.45 mm; $p = 0.0226$) (Fig. 3b).

Table 1 Summary of demographic and clinical characteristics

Characteristic	KMC	ADNI		
	(n = 112)	NC (n = 100)	MCI (n = 100)	AD (n = 100)
M/F	49/63	57/43	69/31	51/49
Age (years old)	46–94	60–90	58–89	57–91
Median age	77	76	76	75
MMSE score	9–30	25–30	24–30	18–27
Median MMSE	26	29	27	23.5

Table 2 Pearson's R and ANOVA with general linear model (GLM) between KMC data and MMSE scores with the FreeSurfer pipeline

	Pearson's R		ANOVA with GLM
	R square	P value	P value
R_entorhinal	0.1682	< 0.0001	0.005*
R_hippocampus	0.1547	< 0.0001	-
Total_hippocampus	0.1423	< 0.0001	-
R_insula	0.1252	0.0001	0.050
R_amygdala	0.1188	0.0002	0.157
L_hippocampus	0.107	0.0004	-

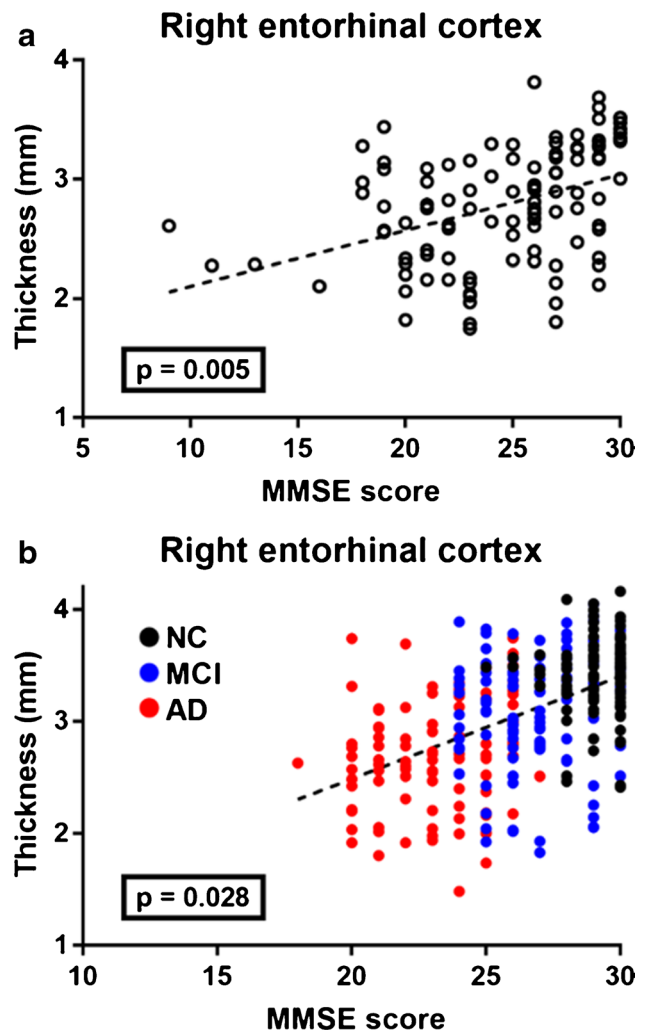Note: *Statistical significance ($p < 0.05$). The underscores represent volume variables

Table 3 Pearson's *R* and ANOVA with GLM between the ADNI data and MMSE score

	Pearson's *R*		ANOVA with GLM
	R square	*P* value	*P* value
L_inferiortemporal	0.2741	< 0.0001	0.111
L_entorhinal	0.2535	< 0.0001	0.487
R_entorhinal	0.2487	< 0.0001	0.039*
L_middletemporal	0.2378	< 0.0001	0.189
R_fusiform	0.2361	< 0.0001	0.035*
L_fusiform	0.221	< 0.0001	0.766
Total hippocampus	0.2153	< 0.0001	0.798
L_hippocampus	0.2122	< 0.0001	0.813
Hippocampus/cerebrum	0.1999	< 0.0001	0.647
R_inferiortemporal	0.1951	< 0.0001	0.998
L_superiortemporal	0.1938	< 0.0001	0.322
R_middletemporal	0.1936	< 0.0001	0.444
L_amygdala	0.1922	< 0.0001	0.448
R_hippocampus	0.189	< 0.0001	-
L_mean cortical thickness	0.1781	< 0.0001	0.36
R_amygdala	0.1741	< 0.0001	0.185
R_inferiorparietal	0.1675	< 0.0001	0.492
R_mean cortical thickness	0.1593	< 0.0001	0.159
L_inferiorparietal	0.1584	< 0.0001	0.025*
L_temporalpole	0.158	< 0.0001	0.81
R_superiortemporal	0.1571	< 0.0001	0.87
L_parahippocampal	0.1418	< 0.0001	0.023*
R_banks of superior temporal sulcus	0.136	< 0.0001	0.479
L_banks of superior temporal sulcus	0.1231	< 0.0001	0.677
R_temporalpole	0.1205	< 0.0001	0.503
L_precuneus	0.118	< 0.0001	0.19
L_medialorbitofrontal	0.1169	< 0.0001	0.623
R_insula	0.1098	< 0.0001	0.646
L_insula	0.1091	< 0.0001	0.256
R_precuneus	0.1067	< 0.0001	0.643
L_supramarginal	0.1055	< 0.0001	0.397
R_medialorbitofrontal	0.0994	< 0.0001	0.568
R_superiorfrontal	0.0951	< 0.0001	0.537
R_caudalmiddlefrontal	0.0938	< 0.0001	0.633
R_rostralmiddlefrontal	0.0924	< 0.0001	0.315
L_isthmuscingulate	0.0909	< 0.0001	0.675

Note: *Statistical significance (*p* < 0.05). The underscores represent volume variables

ERC thickness among normal control, MCI, and AD

The right ERC was thickest with normal control (mean = 3.41 ± 0.47 mm), followed by MCI (mean = 3.08 ± 0.53 mm) and AD (mean = 2.73 ± 0.50 mm; *p* < 0.0001, each) in descending order (Fig. 4a). The left ERC was also the

a Right entorhinal cortex

p = 0.005

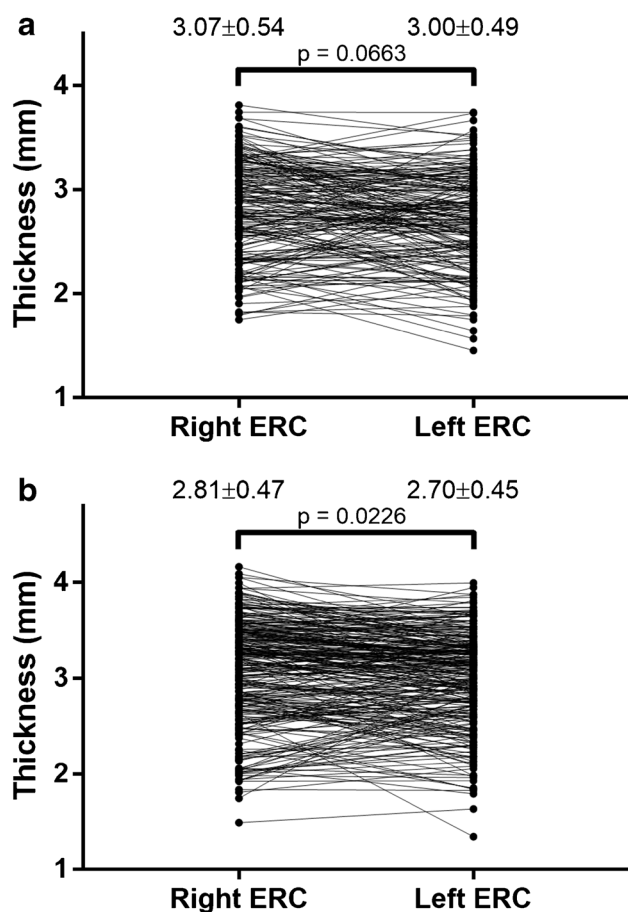**b Right entorhinal cortex**

● NC
● MCI
● AD

p = 0.028

Fig. 2 Scatter plots and linear regression lines of the right ERC thickness from National Hospital Organization Kyushu Medical Center (KMC; **a**) and the ADNI dataset (**b**). GLM analysis demonstrated that right ERC thickness correlated positively with MMSE scores for the first dataset (*p* = 0.005), and thickness of the right ERC (*p* = 0.039) for the ADNI dataset. NC, MCI, and AD represent normal control, mild cognitive impairment (MCI), and Alzheimer's disease, respectively.

thickest with normal control (mean = 3.31 ± 0.29 mm), followed by MCI (mean = 3.01 ± 0.45 mm) and AD (mean = 2.67 ± 0.47 mm; *p* < 0.0001, each) in descending order (Fig. 4b). The right ERC was significantly thicker than the left ERC in normal control (*p* = 0.0255), while we found no significant difference between them in MCI (*p* = 0.82) and AD (*p* > 0.99) groups.

Pearson's correlation coefficients of the dataset from KMC with the ASHS-PMC-T1 pipeline

Variables with moderate correlation coefficients (*r* > 0.3) were volumes of the right anterior/posterior hippocampi,

Fig. 3 Differences in the right and left ERC thickness from KMC (**a**) and the ADNI dataset (**b**). The right ERC tended to be thicker than the left ERC, although no significant difference ($p = 0.0663$) was reported from KMC dataset. In the ADNI dataset, the right ERC was significantly thicker than the left ERC ($p = 0.0226$).
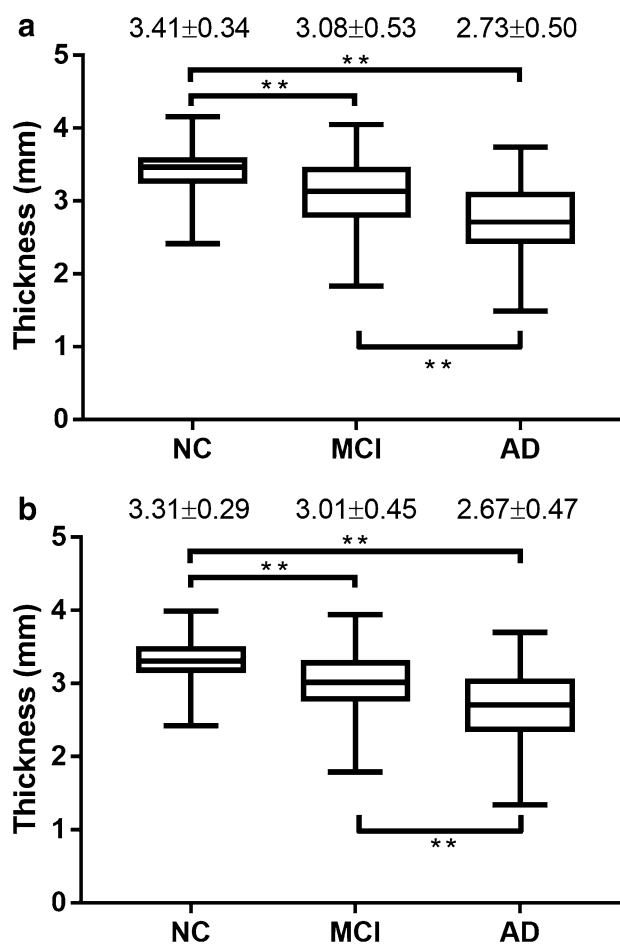
right ERC, left posterior hippocampus, and right BA35 (Table 4). All variables showed positive correlations with MMSE scores.

Fig. 4 Right (**a**) and left ERC (**b**) thicknesses of normal control, MCI, and AD groups. The right ERC was the thickest with normal control (mean = 3.41 ± 0.47 mm), followed by MCI (mean = 3.08 ± 0.53 mm) and AD (mean = 2.73 ± 0.50 mm; $p < 0.0001$, each) in descending order (**a**). The left ERC was also the thickest with normal control (mean = 3.31 ± 0.29 mm), followed by MCI (mean = 3.01 ± 0.45 mm) and AD (mean = 2.67 ± 0.47 mm; $p < 0.0001$, each) in descending order (**b**). The double asterisk indicates $p < 0.0001$

Pearson's correlation coefficients of the dataset from ADNI with the ASHS-PMC-T1 pipeline

Variables with moderate correlation coefficients ($r > 0.3$) were volumes of the right and left anterior/posterior hippocampi, right and left ERC, right and left BA35, right and left BA 36, and left PHC (Table 5). All variables displayed positive correlations with MMSE scores.

GLM analysis of both datasets with the ASHS-PMC-T1 pipeline

GLM analysis demonstrated that no variable correlated significantly with MMSE score for the first dataset (Table 4), while volumes of the left posterior hippocampus ($p = 0.023$)

and left BA36 ($p = 0.012$; Table 5) had significant correlation with MMSE score for the ADNI dataset.

Table 4 Pearson's *R* and ANOVA with GLM between KMC data and MMSE scores with the ASHS-PMC-T1 pipeline

	Pearson's *R*		ANOVA with GLM
	R square	*P* value	*P* value
R_posterior hippocampus	0.136	< 0.0001	0.418
R_ERC	0.1279	0.0001	0.416
L_posterior hippocampus	0.1121	0.0003	0.730
R_anterior hippocampus	0.1019	0.0006	0.598
R_BA35	0.0924	0.0011	0.841

Table 5 Pearson's *R* and ANOVA with GLM between the ADNI data and MMSE score with the ASHS-PMC-T1 pipeline

	Pearson's *R*		ANOVA with GLM
	R square	*P* value	*P* value
L_posterior hippocampus	0.2217	< 0.0001	0.023*
R_posterior hippocampus	0.1727	< 0.0001	0.874
L_ERC	0.1708	< 0.0001	0.174
L_BA36	0.1445	< 0.0001	0.012*
R_ERC	0.1366	< 0.0001	0.793
L_BA35	0.1365	<0.0001	0.541
L_anterior hippocampus	0.1363	< 0.0001	0.789
R_BA35	0.1221	< 0.0001	0.207
R_anterior hippocampus	0.1166	< 0.0001	0.666
L_PHC	0.0964	< 0.0001	0.630

Note: *Statistical significance ($p < 0.05$)

ERC volume among normal control, MCI, and AD

The right ERC was the largest with normal control (mean = 574 ± 92.4 mm^3), followed by MCI (mean = 503 ± 116 mm^3; $p < 0.0001$) and AD (mean = 451 ± 107 mm^3; $p = 0.0017$) in descending order (Fig. 5a). The left ERC was largest with normal control (mean = 586 ± 98.7 mm^3), followed by MCI (mean = 491 ± 118 mm^3; $p < 0.0001$) and AD (mean = 439 ± 118 mm^3; $p = 0.0036$) in descending order (Fig. 5b).

Discussion

Thickness of the right ERC was the common variable which was significantly associated with MMSE score using multi-country datasets in this study. The ERC is pivotally involved in working memory and spatial information [30–32], and mediates the interactions of memory consolidation between the hippocampus and neocortex [31]. Microscopically, grid cells are spatially modulated neurons that have been identified in and around the ERC in mammalian species [33]. Grid cells in the medial ERC generate metric spatial representations [34] and are part of a spatial coordinate system [35]. The ERC is thus the hub of a widespread brain network for navigation and spatial memory [31, 32, 35, 36]. ERC volume [19, 37] and thickness [11, 12, 14–17, 38] are reportedly associated with progression of AD. MMSE scores have been widely used to assess cognitive function. Moreover, the domain of spatial orientation and memory contributes a large proportion of potential points [39]. Taken together, ERC may play key roles in spatial orientation and memory, and MMSE scores appear reasonable to predict thickness of the ERC.

Fig. 5 Right (**a**) and left ERC (**b**) volumes of normal control, MCI, and AD groups. The right ERC was the largest with normal control (mean = 574 ± 92.4 mm^3), followed by MCI (mean = 503 ± 116 mm^3; $p < 0.0001$) and AD (mean = 451 ± 107 mm^3; $p = 0.0017$) in descending order (**a**). The left ERC was largest with normal control (mean = 586 ± 98.7 mm^3), followed by MCI (mean = 491 ± 118 mm^3; $p < 0.0001$) and AD (mean = 439 ± 118 mm^3; $p = 0.0036$) in descending order (**b**). The single and double asterisks indicate $p < 0.01$ and $p < 0.0001$, respectively.

The right ERC tended to be thicker than the left ERC in both datasets. Asymmetry of the cortical thickness reportedly correlates with cognitive function [40]. Previous research has suggested that the volume of the right ERC is greater than that of the left ERC in both normal subjects and patients with AD [37]. Volume of the right ERC was significantly associated with progression of MCI to AD [41]. The apolipoprotein E (ApoE) ε4 allele is a well-established risk factor for AD [42]. Juottonen et al. suggested that the ApoE ε4 allele contributes to atrophy, particularly for the right ERC [37]. That study showed an association between ApoE ε4 allele and neuropathological findings such as increased amyloid plaques and neurofibrillary tangles. Interestingly, the right ERC was significantly thicker than the left ERC in normal control, while we found no significant difference

between them in MCI and AD groups. The loss of asymmetry in ERC has been shown as biomarkers to identify preclinical AD [19], and our findings are in line with the literature. These findings in our study highlighted that the difference in right ERC thickness might be more prominent than that of the left ERC, or the right ERC may play a crucial role in cognitive function.

Thicknesses of the left parahippocampal gyrus, left inferior parietal lobe, and right fusiform gyrus for the ADNI dataset significantly correlated with MMSE scores in GLM analyses from the ADNI dataset, but significantly correlated with MMSE scores only in Pearson's correlation coefficients from the dataset at KMC. It has been reported that volume of the left parahippocampal gyrus is indicative of early biomarker of AD [43]. Some genetic variations might influence the atrophy rates of parahippocampal gyrus [44]. Mental representations are processed within the inferior parietal lobule [45]. Mental representation could be influenced by racial-ethnic group differences in individualism and collectivism [46]. Right fusiform gyrus is involved in face perception, and damage to the right fusiform gyrus resulted in the impairments to normal face recognition [47]. The difference in correlations between thickness of the right fusiform gyrus and MMSE scores from the two datasets might be reduced by perceptual training for other race effects [48], but this issue is beyond scope of the present study. We also observed that volumes of the left posterior hippocampus and left BA36 had significant correlation with MMSE score from the ADNI dataset. Similar findings have been reported in patients with early stages of AD [13, 49]. BA36 has been reportedly associated with personality changes such as agreeableness and openness [50]. These personality changes might influence the discrepancy on the GLM analysis between the two datasets in our study.

In Pearson's correlation coefficients, more variables including hippocampus volume were associated with MMSE scores in our study. A plethora of evidence has suggested that hippocampus volume is closely related to cognitive function. Our results provide informative data to help discern the correlations between volume of the hippocampus and MMSE scores in a non-invasive manner.

To obtain common characteristics from multi-country datasets, the preprocessing pipeline needs to be taken into consideration regarding morphological differences between various races and ethnicities across multi-country datasets. The FreeSurfer pipeline has been used worldwide to acquire quantitative variables in the brain [22]. Discovery of a common variable from multi-country datasets appears reasonable for understanding how MMSE scores are influenced by the thickness of the right ERC. In summary, the present study may allow non-invasive creation of predictive models in multi-country datasets non-invasively.

Our study has several limitations. First, handedness data was unavailable and thus might have influenced the laterality result. However, the volume of the right ERC is reportedly larger than left ERC volume in both normal subjects and patients with AD [37]. This study did not take into account the potential for differences in the questionnaire or detailed rating scales between MMSE and MMSE-J. Lastly, MR images were acquired on a 1.5-T unit in the present study. Xie et al. proposed the ASHS-PMC-T1 pipeline without T2-weighted images [13] although the combination of T1- and coronal T2-weighted images using a 3.0-T unit may provide better segmentation results when analyzing MTL subfield.

In conclusion, we found the positive correlations between right ERC thickness and MMSE scores using multi-country datasets. Computing right ERC thickness may be a potential option in patients with cognitive impairment without regard to race or ethnicity.

Declarations

References

1. Braak H, Braak E (1995) Staging of Alzheimer's disease-related neurofibrillary changes. Neurobiol Aging 16:271–278; discussion 278-284. https://doi.org/10.1016/0197-4580(95)00021-6
2. Squire LR, Zola-Morgan S (1991) The medial temporal lobe memory system. Science 253:1380–1386. https://doi.org/10.1126/science.1896849
3. Thaker AA, Weinberg BD, Dillon WP, Hess CP, Cabral HJ, Fleischman DA, Leurgans SE, Bennett DA, Hyman BT, Albert MS, Killiany RJ, Fischl B, Dale AM, Desikan RS (2017) Entorhinal cortex: antemortem cortical thickness and postmortem neurofibrillary tangles and amyloid pathology. AJNR Am J Neuroradiol 38:961–965. https://doi.org/10.3174/ajnr.A5133
4. Vermersch P, Frigard B, David JP, Fallet-Bianco C, Delacourte A (1992) Presence of abnormally phosphorylated Tau proteins in the entorhinal cortex of aged non-demented subjects. Neurosci Lett 144:143–146. https://doi.org/10.1016/0304-3940(92)90736-q
5. Knopman DS, Lundt ES, Therneau TM, Vemuri P, Lowe VJ, Kantarci K, Gunter JL, Senjem ML, Mielke MM, Machulda MM, Boeve BF, Jones DT, Graff-Radford J, Albertson SM, Schwarz CG, Petersen RC, Jack CR (2019) Entorhinal cortex tau, amyloid-beta, cortical thickness and memory performance in nondemented subjects. Brain 142:1148–1160. https://doi.org/10.1093/brain/awz025
6. Kordower JH, Chu Y, Stebbins GT, DeKosky ST, Cochran EJ, Bennett D, Mufson EJ (2001) Loss and atrophy of layer II entorhinal cortex neurons in elderly people with mild cognitive impairment. Ann Neurol 49:202–213
7. Meunier M, Bachevalier J, Mishkin M, Murray EA (1993) Effects on visual recognition of combined and separate ablations of the entorhinal and perirhinal cortex in rhesus monkeys. J Neurosci 13:5418–5432
8. Han X, Jovicich J, Salat D, van der Kouwe A, Quinn B, Czanner S, Busa E, Pacheco J, Albert M, Killiany R, Maguire P, Rosas D, Makris N, Dale A, Dickerson B, Fischl B (2006) Reliability of MRI-derived measurements of human cerebral cortical thickness: the effects of field strength, scanner upgrade and manufacturer. NeuroImage 32:180–194. https://doi.org/10.1016/j.neuroimage.2006.02.051
9. Dickerson BC, Fenstermacher E, Salat DH, Wolk DA, Maguire RP, Desikan R, Pacheco J, Quinn BT, Van der Kouwe A, Greve DN, Blacker D, Albert MS, Killiany RJ, Fischl B (2008) Detection of cortical thickness correlates of cognitive performance: reliability across MRI scan sessions, scanners, and field strengths. NeuroImage 39:10–18. https://doi.org/10.1016/j.neuroimage.2007.08.042
10. Dick JP, Guiloff RJ, Stewart A, Blackstock J, Bielawska C, Paul EA, Marsden CD (1984) Mini-mental state examination in neurological patients. J Neurol Neurosurg Psychiatry 47:496–499. https://doi.org/10.1136/jnnp.47.5.496
11. Velayudhan L, Proitsi P, Westman E, Muehlboeck JS, Mecocci P, Vellas B, Tsolaki M, Kloszewska I, Soininen H, Spenger C, Hodges A, Powell J, Lovestone S, Simmons A, dNeuroMed C, (2013) Entorhinal cortex thickness predicts cognitive decline in Alzheimer's disease. J Alzheimers Dis 33:755–766. https://doi.org/10.3233/JAD-2012-121408
12. Krumm S, Kivisaari SL, Probst A, Monsch AU, Reinhardt J, Ulmer S, Stippich C, Kressig RW, Taylor KI (2016) Cortical thinning of parahippocampal subregions in very early Alzheimer's disease. Neurobiol Aging 38:188–196. https://doi.org/10.1016/j.neurobiolaging.2015.11.001
13. Xie L, Wisse LEM, Pluta J, de Flores R, Piskin V, Manjon JV, Wang H, Das SR, Ding SL, Wolk DA, Yushkevich PA, Alzheimer's Disease Neuroimaging I, (2019) Automated segmentation of medial temporal lobe subregions on in vivo T1-weighted MRI in early stages of Alzheimer's disease. Hum Brain Mapp 40:3431–3451. https://doi.org/10.1002/hbm.24607
14. Curiel RE, Loewenstein DA, Rosselli M, Penate A, Greig-Custo MT, Bauer RM, Guinjoan SM, Hanson KS, Li C, Lizarraga G, Barker WW, Torres V, DeKosky S, Adjouadi M, Duara R (2018) Semantic intrusions and failure to recover from semantic interference in mild cognitive impairment: relationship to amyloid and cortical thickness. Curr Alzheimer Res 15:848–855. https://doi.org/10.2174/1567205015666180427122746
15. Harrison TM, Mahmood Z, Lau EP, Karacozoff AM, Burggren AC, Small GW, Bookheimer SY (2016) An Alzheimer's disease genetic risk score predicts longitudinal thinning of hippocampal complex subregions in healthy older adults. eNeuro 3.https://doi.org/10.1523/ENEURO.0098-16.2016
16. Arruda F, Rosselli M, Greig MT, Loewenstein DA, Lang M, Torres VL, Velez-Uribe I, Conniff J, Barker WW, Curiel RE, Adjouadi M, Duara R (2021) The association between functional assessment and structural brain biomarkers in an ethnically diverse sample with normal cognition, mild cognitive impairment, or dementia. Arch Clin Neuropsychol 36:51–61. https://doi.org/10.1093/arclin/acaa065
17. Li S, Yuan X, Pu F, Li D, Fan Y, Wu L, Chao W, Chen N, He Y, Han Y (2014) Abnormal changes of multidimensional surface features using multivariate pattern classification in amnestic mild cognitive impairment patients. J Neurosci 34:10541–10553. https://doi.org/10.1523/JNEUROSCI.4356-13.2014
18. Yamashita K, Kuwashiro T, Ishikawa K, Furuya K, Harada S, Shin S, Wada N, Hirakawa C, Okada Y, Noguchi T (2021) Identification of predictors for mini-mental state examination and revised Hasegawa's Dementia Scale scores using MR-based brain morphometry. Eur J Radiol Open 8:100359. https://doi.org/10.1016/j.ejro.2021.100359
19. Long X, Zhang L, Liao W, Jiang C, Qiu B, Alzheimer's Disease Neuroimaging I, (2013) Distinct laterality alterations distinguish mild cognitive impairment and Alzheimer's disease from healthy aging: statistical parametric mapping with high resolution MRI. Hum Brain Mapp 34:3400–3410. https://doi.org/10.1002/hbm.22157
20. Mueller SG, Weiner MW, Thal LJ, Petersen RC, Jack C, Jagust W, Trojanowski JQ, Toga AW, Beckett L (2005) The Alzheimer's disease neuroimaging initiative. Neuroimaging Clin N Am 15(869–877):xi–xii. https://doi.org/10.1016/j.nic.2005.09.008
21. Fischl B, Salat DH, Busa E, Albert M, Dieterich M, Haselgrove C, van der Kouwe A, Killiany R, Kennedy D, Klaveness S, Montillo A, Makris N, Rosen B, Dale AM (2002) Whole brain segmentation: automated labeling of neuroanatomical structures in the human brain. Neuron 33:341–355. https://doi.org/10.1016/s0896-6273(02)00569-x
22. Fischl B (2012) FreeSurfer. NeuroImage 62:774–781. https://doi.org/10.1016/j.neuroimage.2012.01.021
23. Desikan RS, Segonne F, Fischl B, Quinn BT, Dickerson BC, Blacker D, Buckner RL, Dale AM, Maguire RP, Hyman BT, Albert MS, Killiany RJ (2006) An automated labeling system for subdividing the human cerebral cortex on MRI scans into gyral based regions of interest. NeuroImage 31:968–980. https://doi.org/10.1016/j.neuroimage.2006.01.021
24. Otsuka Y, Kakeda S, Sugimoto K, Katsuki A, Nguyen LH, Igata R, Watanabe K, Ueda I, Kishi T, Iwata N, Korogi Y, Yoshimura R (2019) COMT polymorphism regulates the hippocampal subfield volumes in first-episode, drug-naive patients with major depressive disorder. Neuropsychiatr Dis Treat 15:1537–1545. https://doi.org/10.2147/NDT.S199598
25. Yushkevich PA, Pluta JB, Wang H, Xie L, Ding SL, Gertje EC, Mancuso L, Kliot D, Das SR, Wolk DA (2015) Automated

volumetry and regional thickness analysis of hippocampal subfields and medial temporal cortical structures in mild cognitive impairment. Hum Brain Mapp 36:258–287. https://doi.org/10.1002/hbm.22627

26. Yushkevich PA, Piven J, Hazlett HC, Smith RG, Ho S, Gee JC, Gerig G (2006) User-guided 3D active contour segmentation of anatomical structures: significantly improved efficiency and reliability. NeuroImage 31:1116–1128. https://doi.org/10.1016/j.neuroimage.2006.01.015

27. Hawkins DM (2004) The problem of overfitting. J Chem Inf Comput Sci 44:1–12. https://doi.org/10.1021/ci0342472

28. Zhang Z (2014) Too much covariates in a multivariable model may cause the problem of overfitting. J Thorac Dis 6:E196-197. https://doi.org/10.3978/j.issn.2072-1439.2014.08.33

29. Ratner B (2009) The correlation coefficient: its values range between +1/−1, or do they? Journal of Targeting, Measurement and Analysis for Marketing 17:139–142. https://doi.org/10.1057/jt.2009.5

30. Egorov AV, Hamam BN, Fransen E, Hasselmo ME, Alonso AA (2002) Graded persistent activity in entorhinal cortex neurons. Nature 420:173–178. https://doi.org/10.1038/nature01171

31. Fyhn M, Molden S, Witter MP, Moser EI, Moser MB (2004) Spatial representation in the entorhinal cortex. Science 305:1258–1264. https://doi.org/10.1126/science.1099901

32. Hafting T, Fyhn M, Molden S, Moser MB, Moser EI (2005) Microstructure of a spatial map in the entorhinal cortex. Nature 436:801–806. https://doi.org/10.1038/nature03721

33. Moser EI, Roudi Y, Witter MP, Kentros C, Bonhoeffer T, Moser MB (2014) Grid cells and cortical representation. Nat Rev Neurosci 15:466–481. https://doi.org/10.1038/nrn3766

34. Buetfering C, Allen K, Monyer H (2014) Parvalbumin interneurons provide grid cell-driven recurrent inhibition in the medial entorhinal cortex. Nat Neurosci 17:710–718. https://doi.org/10.1038/nn.3696

35. Sargolini F, Fyhn M, Hafting T, McNaughton BL, Witter MP, Moser MB, Moser EI (2006) Conjunctive representation of position, direction, and velocity in entorhinal cortex. Science 312:758–762. https://doi.org/10.1126/science.1125572

36. Quirk GJ, Muller RU, Kubie JL, Ranck JB Jr (1992) The positional firing properties of medial entorhinal neurons: description and comparison with hippocampal place cells. J Neurosci 12:1945–1963

37. Juottonen K, Lehtovirta M, Helisalmi S, Riekkinen PJ Sr, Soininen H (1998) Major decrease in the volume of the entorhinal cortex in patients with Alzheimer's disease carrying the apolipoprotein E epsilon4 allele. J Neurol Neurosurg Psychiatry 65:322–327. https://doi.org/10.1136/jnnp.65.3.322

38. Donix M, Burggren AC, Scharf M, Marschner K, Suthana NA, Siddarth P, Krupa AK, Jones M, Martin-Harris L, Ercoli LM, Miller KJ, Werner A, von Kummer R, Sauer C, Small GW, Holthoff VA, Bookheimer SY (2013) APOE associated hemispheric asymmetry of entorhinal cortical thickness in aging and Alzheimer's disease. Psychiatry Res 214:212–220. https://doi.org/10.1016/j.pscychresns.2013.09.006

39. Shigemori K, Ohgi S, Okuyama E, Shimura T, Schneider E (2010) The factorial structure of the Mini-Mental State Examination (MMSE) in Japanese dementia patients. BMC Geriatr 10:36. https://doi.org/10.1186/1471-2318-10-36

40. Chen C, Omiya Y (2014) Brain asymmetry in cortical thickness is correlated with cognitive function. Front Hum Neurosci 8:877. https://doi.org/10.3389/fnhum.2014.00877

41. Tapiola T, Pennanen C, Tapiola M, Tervo S, Kivipelto M, Hanninen T, Pihlajamaki M, Laakso MP, Hallikainen M, Hamalainen A, Vanhanen M, Helkala EL, Vanninen R, Nissinen A, Rossi R, Frisoni GB, Soininen H (2008) MRI of hippocampus and entorhinal cortex in mild cognitive impairment: a follow-up study. Neurobiol Aging 29:31–38. https://doi.org/10.1016/j.neurobiolaging.2006.09.007

42. Choudhury P, Ramanan VK, Boeve BF (2021) APOE varepsilon4 allele testing and risk of Alzheimer disease. JAMA 325:484–485. https://doi.org/10.1001/jama.2020.15085

43. Echavarri C, Aalten P, Uylings HB, Jacobs HI, Visser PJ, Gronenschild EH, Verhey FR, Burgmans S (2011) Atrophy in the parahippocampal gyrus as an early biomarker of Alzheimer's disease. Brain Struct Funct 215:265–271. https://doi.org/10.1007/s00429-010-0283-8

44. Wang WY, Liu Y, Wang HF, Tan L, Sun FR, Tan MS, Tan CC, Jiang T, Tan L, Yu JT, Alzheimer's Disease Neuroimaging I, (2017) Impacts of CD33 genetic variations on the atrophy rates of hippocampus and parahippocampal gyrus in normal aging and mild cognitive impairment. Mol Neurobiol 54:1111–1118. https://doi.org/10.1007/s12035-016-9718-4

45. Jancke L, Kleinschmidt A, Mirzazade S, Shah NJ, Freund HJ (2001) The role of the inferior parietal cortex in linking the tactile perception and manual construction of object shapes. Cereb Cortex 11:114–121. https://doi.org/10.1093/cercor/11.2.114

46. Hawkley LC, Gu Y, Luo YJ, Cacioppo JT (2012) The mental representation of social connections: generalizability extended to Beijing adults. PloS one 7:e44065. https://doi.org/10.1371/journal.pone.0044065

47. Susilo T, Yang H, Potter Z, Robbins R, Duchaine B (2015) Normal body perception despite the loss of right fusiform gyrus. J Cogn Neurosci 27:614–622. https://doi.org/10.1162/jocn_a_00743

48. Heron-Delaney M, Anzures G, Herbert JS, Quinn PC, Slater AM, Tanaka JW, Lee K, Pascalis O (2011) Perceptual training prevents the emergence of the other race effect during infancy. PloS one 6:e19858. https://doi.org/10.1371/journal.pone.0019858

49. Ogawa M, Sone D, Beheshti I, Maikusa N, Okita K, Takano H, Matsuda H (2019) Association between subfield volumes of the medial temporal lobe and cognitive assessments. Heliyon 5:e01828. https://doi.org/10.1016/j.heliyon.2019.e01828

50. Kapogiannis D, Sutin A, Davatzikos C, Costa P Jr, Resnick S (2013) The five factors of personality and regional cortical variability in the Baltimore longitudinal study of aging. Hum Brain Mapp 34:2829–2840. https://doi.org/10.1002/hbm.22108